RICCAR

Regional Initiative for the Assessment of Climate Change Impacts on Water Resources and Socio-Economic Vulnerability in the Arab Region

Impact of Climate Change on Extreme Events in Selected Basins in the Arab Region

TECHNICAL REPORT

THE LEAGUE OF ARAB STATES
THE ARAB CENTER FOR THE STUDIES OF ARID ZONES AND DRY LANDS
ACSAD 1968 أكساد

UNITED NATIONS
الاسكوا
ESCWA

RICCAR

Regional Initiative for the Assessment of Climate Change Impacts on Water Resources and Socio-Economic Vulnerability in the Arab Region

Impact of Climate Change on Extreme Events in Selected Basins in the Arab Region

Regional Initiative for the Assessment of Climate Change Impacts on Water Resources and Socio-Economic Vulnerability in the Arab Region

TECHNICAL REPORT

Arab Center for the Studies of Arid Zones and Dry Lands (ACSAD)

United Nations Economic and Social Commission for Western Asia (ESCWA)

Email: publications-escwa@un.org
Website: www.unescwa.org; www.riccar.org

Available through:
United Nations Publication
E/ESCWA/SDPD/2017/RICCAR/TechnicalReport.5

Reference as:
Arab Center for the Studies of Arid Zones and Dry Lands (ACSAD) and United Nations Economic and Social Commission for Western Asia (ESCWA). 2017. Impact of Climate Change on Extreme Events in Selected Basins in the Arab Region. RICCAR Technical Report, Beirut, E/ESCWA/SDPD/2017/RICCAR/TechnicalReport.5.

Authors:
Arab Center for the Studies of Arid Zones and Dry Lands (ACSAD)
United Nations Economic and Social Commission for Western Asia (ESCWA)

Layout: Ghazal Lababidi

PREFACE

The Regional Initiative for the Assessment of Climate Change Impacts on Water Resources and Socio-Economic Vulnerability in the Arab Region (RICCAR) is a joint initiative of the United Nations and the League of Arab States launched in 2010.

RICCAR is implemented through a collaborative partnership involving 11 regional and specialized organizations, namely the United Nations Economic and Social Commission for Western Asia (ESCWA), Arab Center for the Studies of Arid Zones and Dry Lands (ACSAD), Food and Agriculture Organization of the United Nations (FAO), Deutsche Gesellschaft für Internationale Zusammenarbeit (GIZ), League of Arab States, Swedish Meteorological and Hydrological Institute (SMHI), United Nations Environment Programme (UN Environment), United Nations Educational, Scientific and Cultural Organization (UNESCO) Office in Cairo, United Nations Office for Disaster Risk Reduction (UNISDR), United Nations University Institute for Water, Environment and Health (UNU-INWEH), and World Meteorological Organization (WMO). ESCWA coordinates the regional initiative. Funding for RICCAR is provided by the Government of Sweden and the Government of the Federal Republic of Germany.

RICCAR is implemented under the auspices of the Arab Ministerial Water Council and derives its mandate from resolutions adopted by this council as well as the Council of Arab Ministers Responsible for the Environment, the Arab Permanent Committee for Meteorology and the 25th ESCWA Ministerial Session.

CONTENTS

FIGURES

TABLES

ACRONYMS AND ABBREVIATIONS

AR5	Fifth Assessment Report (IPCC)
CAMRE	Council of Arab Ministers Responsible for the Environment
CDD	maximum length of dry spell
CNRM-CM5	Centre National de Recherches Météorologiques- Climate Model 5
CO_2	carbon dioxide
CSDI	cold spell duration index
CWD	maximum length of wet spell
EC-EARTH	ECMWF-based Earth-system model
ESCWA	United Nations Economic and Social Commission for Western Asia
ETCCDI	Expert Team on Climate Change Detection and Indices
GCM	global climate model or general circulation model
GFDL-ESM2M	Geophysical Fluid Dynamics Laboratory-Earth System Model 2
GIS	Geographic Information Systems
HEC-HMS	Hydrologic Engineering Center Hydrological Modelling System (hydrological model)
IPCC	Intergovernmental Panel on Climate Change
km	kilometres
km^2	square kilometres
m asl	metres above sea level
mm	millimetres
mm/yr	millimetres per year
m^3/s	cubic metre per second
ppm	parts per million
RCA4	Rossby Centre Regional Atmospheric Model 4
RCM	regional climate model
RCP	representative concentration pathway
RHM	regional hydrological model
RICCAR	Regional Initiative for the Assessment of Climate Change Impacts on Water Resources and Socio-Economic Vulnerability in the Arab Region
R10	annual number of days with precipitation greater than 10 mm
R20	annual number of days with precipitation greater than 20 mm
SDII	simple daily intensity index
SMA	Soil Moisture Accounting
SMHI	Swedish Meteorological and Hydrological Institute
SPI	standardized precipitation index
SU35	number of hot days
SU40	number of very hot days
TR	tropical nights
WMO	World Meteorological Organization
WSDI	warm spell duration index
°C	degree Celsius
%	per cent

EXECUTIVE SUMMARY

A case study examined the impacts of climate change in terms of extreme events in three river basins in the Arab region, namely the Nahr el Kabir River basin shared between Lebanon and the Syrian Arab Republic; the Wadi Diqah River basin in Oman; and the Medjerda River basin shared between Algeria and Tunisia. For each basin, changes in the following indicators were analysed: extreme temperature and precipitation indices, extreme drought events and extreme flood events. Three time periods were selected for presenting results, consisting of a reference period (1986–2005), a mid-century period (2046–2065), and an end-century period (2081–2100). Two different emission scenarios were considered namely RCP 4.5 and RCP 8.5.

The extreme events studied include 10 indices selected from the WMO Expert Team on Climate Change Detection and Indices (ETCCDI) indicators, and were based on processing of Regional Climate Modelling (RCM) temperature and precipitation projections generated under RICCAR, into indices of climate extremes using the RClimDex package.

Extreme droughts were assessed using the Standardized Precipitation Index–SPI method based on RICCAR precipitation time series according to the different SPI timescales selected: six-month SPI and 12-month SPI.

Changes in the magnitude and frequency of extreme streamflow events were investigated through an analysis of flood events exceeding the 90th percentile of the maximum daily value, as well as changes in the frequency of extreme flows with return periods equal or larger than 100 years. Extreme flood events were examined by performing hydrological modelling runs using the Hydrologic Engineering Center Hydrological Modelling System (HEC-HMS) model and the ArcGIS extension HEC-GeoHMS.

Results have shown that all three basins are projected to experience increases in heat extremes by the end of the century and for both emission scenarios. Projections for precipitation extremes are more variable, with a general increasing trend in consecutive dry days (CDD) for the selected basins in most cases, coupled to an increasing trend in 20 mm precipitation days (R20) by the end of the century for all basins except for the Medjerda River.

Concerning drought and flood events, the following results have been reported:

For the **Nahr el Kabir basin**, a tendency towards drier conditions is projected by end-century with an increase in the occurrence of moderate drought in particular for RCP 8.5, but with no severe or extreme droughts events projected to occur. The basin is likely to experience an increase in the magnitude of peak flow and flood frequencies over the 21st century.

For the **Wadi Diqah basin**, in accordance with the reference period, there is no indication of projected severe or extreme droughts over the 21st century, while moderate drought conditions are still projected to occur with generally few changes compared to the reference period. The magnitude of peak flow events is likely to increase in the basin by the end of the century, and projections show a decreasing number of extreme flood days at mid-century, followed by an increase at end-century.

For the **Medjerda basin**, there is a tendency towards significantly drier conditions with projected episodes of severe and extreme droughts over time, in addition to moderate drought which is projected for both time periods and emission scenarios. For the moderate emission scenario, the basin is likely to experience an increase in the magnitude of peak flows together with a decreasing number of extreme flood events. For the high-emission scenario, however, the mean magnitude of peak flow is projected to decrease over time.

1 INTRODUCTION AND STUDY SITES

The Arab region is highly vulnerable to extreme events. In the recent past, the region has witnessed a significant rise in the frequency and intensity of heat waves, droughts, and floods which caused immeasurable damage of properties and loss of life. The 1998-2000 drought swept over much of the Arab region and had strong negative impacts on the agriculture sector and on the overall national economies of many Arab States such as Syria and Jordan. Numerous heat records were broken in the region in the summer of 2010 with temperatures reaching 52°C in Jeddah.[1] Moreover, from 2003 to 2017, severe floods affected Saudi Arabia (2013, 2017), Tunisia (2005), Lebanon (2013), and Yemen (2008) resulting in considerable economic losses. Furthermore, the super cyclonic storm, known as hurricane Gonu in 2007 was considered the worst natural disaster on record in Oman, with total rainfall reaching 610 mm near the coast.

Many studies based on a number of global climate modelling (GCM) and regional climate modelling (RCM) projections indicate that climate change could cause an increase in the frequency of extreme weather events, potentially making them more common in the future.[2] Therefore, as climate change intensifies, the Arab region is expected to experience increased extreme weather events. Hence, improving the understanding of climate extremes is important in order to better prepare of adaption measures which could be applied to mitigate potential adverse effects. This can be done by investigating the characteristics of climate extremes, calculating various indices that could be derived from available temperature, precipitation and stream flow data and analyzing past and projected future trends in these extremes.

This study is conducted as part of the Regional Initiative for the Assessment of Climate Change Impacts on Water Resources and Socio-Economic Vulnerability in the Arab Region (RICCAR), whose main goal was to gain insights on the patterns of climatic changes and its impacts on water resources in the Arab region through an integrated assessment. The assessment comprised analysis of changes in climatic and hydrological variables over the region and in selected subdomains, as well as shedding the light on some projected impacts and vulnerabilities on different sectors in the region.[3]

Within RICCAR, climate change data was produced through downscaling projection from three global circulation models; EC-EARTH, CNRM-CM5, and GFDL-ESM2M on a specific Arab Domain using the regional climate model Rossby Centre Regional Atmospheric Model 4 (RCA4) to provide high-resolution information (50x50 km scale). These high-resolution climate outputs were generated for two emission scenarios, namely RCP4.5 and RCP8.5. The availability of long time series of projected climate data of daily time steps offers a great opportunity to evaluate and improve understanding of future impact of climate change on extreme events in the Arab region.

The objective of this study is to investigate the impact of climate change on extreme events on three basins in the Arab region: 1) Nahr El Kabir[4] river basin– in the Syrian Arab Republic and Lebanon, 2) Wadi Diqah river basin – in the Sultanate of Oman, and 3) Medjerda river basin – in Algeria and Tunisia. A wide range of phenomena were considered including temperature and precipitation extremes, drought extremes and hydrological extremes. The following sections provide a brief overview on each of the selected river basins.

FIGURE 1: Extreme events case studies: study area

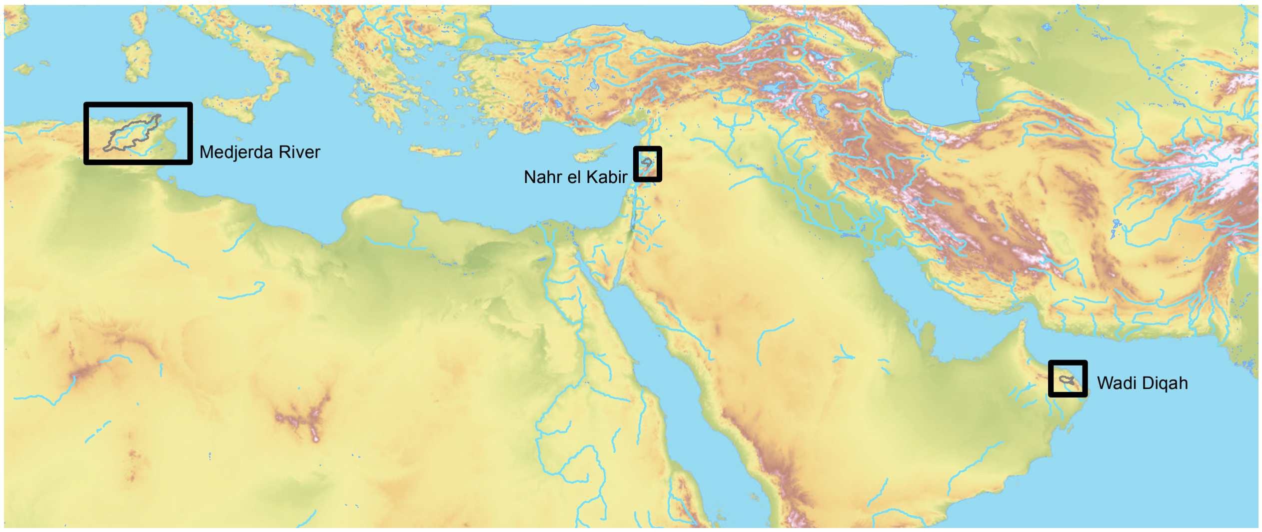

1.1 Nahr el Kabir River Basin

The Nahr el Kabir river is 56 km long and flows along the northern Lebanese border with Syrian Arab Republic. Its total watershed area is about 990 km^2 of which 295 km^2 lies in Lebanon (Figure 2). The basin has an altitude varying between about 1,000-2,300 m asl in the eastern boundary to 0 m asl in the western sea coast, with the most part lying between 100 and 600 m asl. The river collects its water from tributaries on both sides and flows from east to west down to the Mediterranean Sea at its outlet in the Akkar bay, 15 km to the North of the city of Tripoli in Lebanon. The average river basin slope is 12.8%.

FIGURE 2: Location of the Nahr el Kabir River Basin

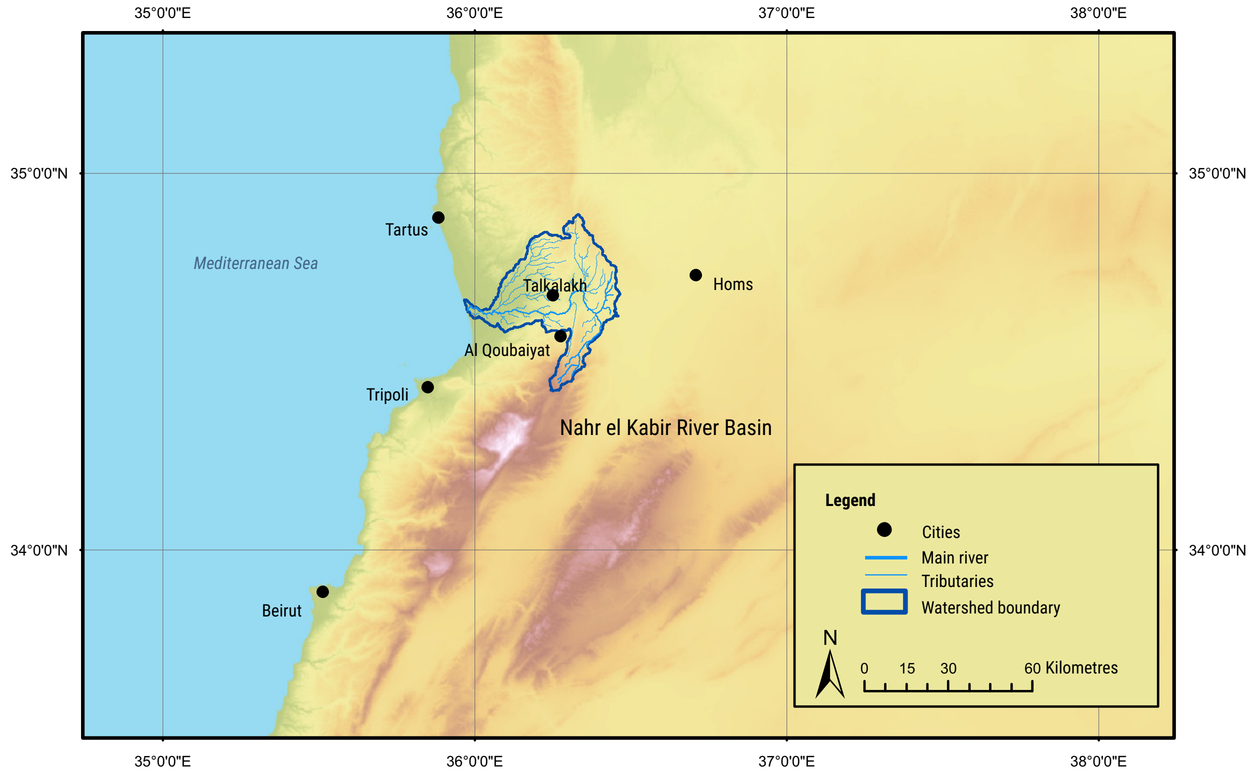

Nahr el Kabir River, Syrian Arab Republic, 2007. Source: Ihab Jnad.

1.2 Wadi Diqah River Basin

The Wadi Diqah river is located 60 km southeast of Muscat (Figure 3) and is one of the few continuously flowing valleys around the year in Oman. The watercourse is 70 km long and the watershed covers a surface area of some 1,870 km^2. The basin is oriented in a west–east direction with an altitude varying between 780 and 1,350 m asl in the western boundary to 0 m asl on the western Gulf coast, with most of the basin area lying between 500 and 700 m asl. The rivercourse extends from the village of Toul till the village of Doghmor, passing through several straits before discharging into the sea. The average basin slope is 28.7%, and rainfall varies seasonally and geographically over the area with an annual average precipitation of about 148 mm/yr (about 276 million m^3).

FIGURE 3: Location of the Wadi Diqah Basin

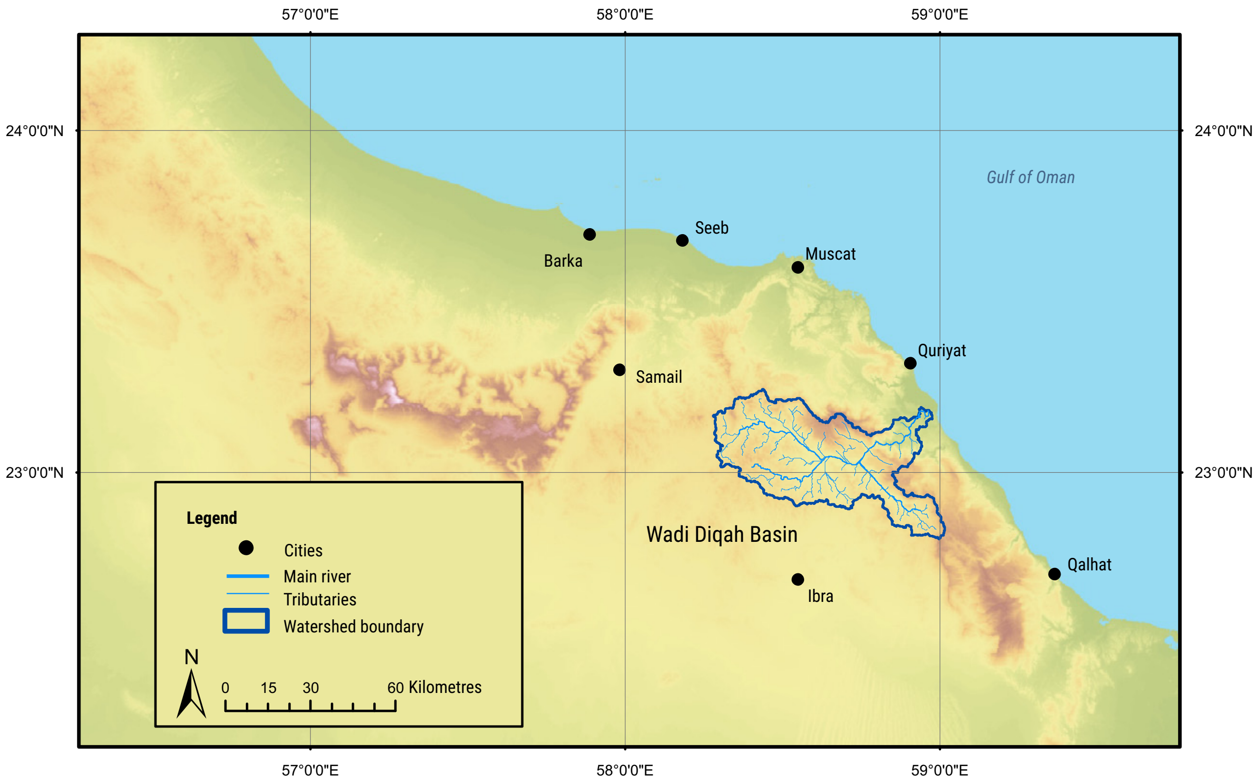

Wadi Diqah Dam reservoir, Oman, 2011. Source: Ihab Jnad.

1.3 Medjerda River Basin

The Medjerda river basin extends from across the border in Algeria up to the Gulf of Utica (Figure 4). Its total watershed area is about 22,700 km^2 of which 450 km^2 lies in Algeria. The basin's topography varies between 2,500 and 3,000 m asl in the western boundary to 0 m asl on the western Gulf coast, with most of the basin area lying between 700 and 2,000 m asl. The main watercourse length is 100 km of which 36 km run in Algeria. It collects its water from tributaries on both sides of the riverbed and flows from west to east down to the Gulf of Utica. The average basin slope is 8.4%. The Medjerda basin area is characterized by a sub-humid to semi-arid climate with a mean annual rainfall of 480 mm/yr in the watershed with irregular patterns in time and in space.

FIGURE 4: Location of the Medjerda River Basin

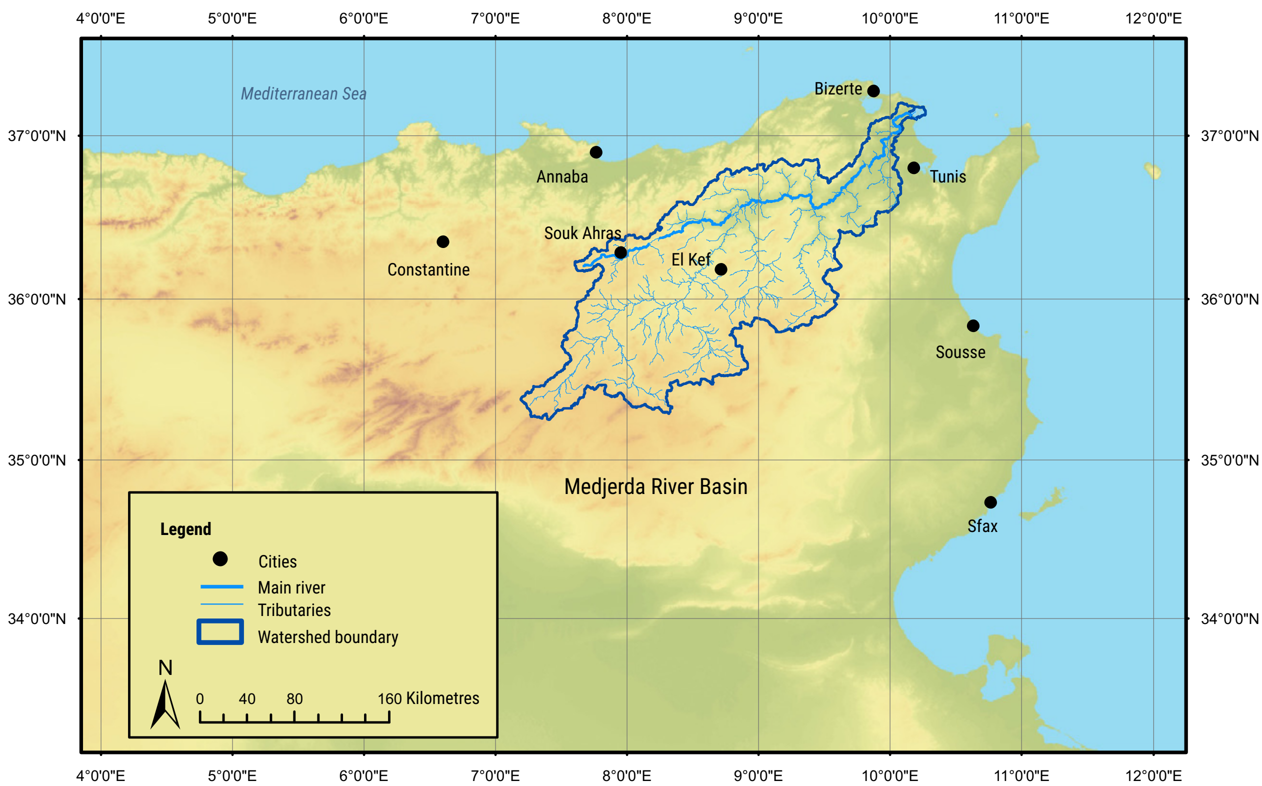

Sidi Salem dam, Medjerda River, Tunisia, 2015. Source: Elarbi Alaeddin.

2 DATA

Datasets used in this assessment comprises a combination of regional climate modelling projections data generated from RICCAR, and a set of observation datasets for precipitation and discharge for the three selected basins. Information on each of these data sources is provided in the following sections.

2.1 Climate change data

Climate change projections in this study were based on two of the four representative concentration pathways (RCPs) or emission scenarios used by the Intergovernmental Panel on Climate Change (IPCC) for informing global and regional climate modelling work presented in its Fifth Assessment Report (AR5).

In line with the work of RICCAR, the two following emission scenarios were used in this assessment:

- RCP 4.5: is a scenario in which radiative forcing is stabilized at 4.5 W/m^2 in the year 2100 without ever exceeding this value (approximately 650 ppm CO_2-equivalent). It generally describes a moderate emissions scenario.
- RCP 8.5: in this scenario, greenhouse gas emissions and concentrations increase considerably over time, leading to a radiative forcing of 8.5 W/m^2 at the end of the century (approximately 1,370 ppm CO_2-equivalent). It is considered as a high emissions or “business as usual” scenario.

Climate change data pertaining to temperature and precipitation projections was obtained from outputs generated under RICCAR. The latter are regional climate modelling datasets that were generated by the Swedish Meteorological and Hydrological Institute (SMHI) using the Rossby Centre Regional Atmospheric Model 4 (RCA4), forced at its boundaries by three state of- the-art global climate models, namely EC-Earth, CNRM and GFDL-ESM.

The outputs were bias-corrected using the distribution-based scaling (DBS) method. An average of the three-model output (“ensemble”) was derived for RCP 4.5 and RCP 8.5 for various climate variables at a horizontal resolution of 50 km and up to the end of the 21st century.[5] The three time periods consist of the following:

- Reference period (1986–2005)
- Mid-century period (2046–2065)
- End-century period (2081–2100).

Characteristics of temperature and precipitation projections stemming from RICCAR regional climate modelling are presented in Table 1.

TABLE 1: Characteristics of RICCAR RCM outputs

Time Period	Emission scenario	Description
Reference period	–	Baseline period representative of 1986-2005
Mid-century	RCP 4.5	Intermediate future scenario representative of the period 2046-2065 and based on RCP 4.5 (moderate impact)
Mid-century	RCP 8.5	Intermediate future scenario representative of the period 2046-2065 and based on RCP 8.5 (extreme impact)
End-century	RCP 4.5	Far future scenario representative of the period 2081-2100 and based on RCP 4.5 (moderate impact)
End-century	RCP 8.5	Far future scenario representative of the period 2081-2100 and based on RCP 8.5 (extreme impact)

Figure 5 shows the change in mean temperature and precipitation over time as a 20-year moving average for the three investigated basins.

FIGURE 5: Mean precipitation (mm/yr) and temperature (°C) over time for the different river basins as a 20-year moving average for six individual climate projections

PRECIPITATION	TEMPERATURE

Nahr el Kabir River Basin

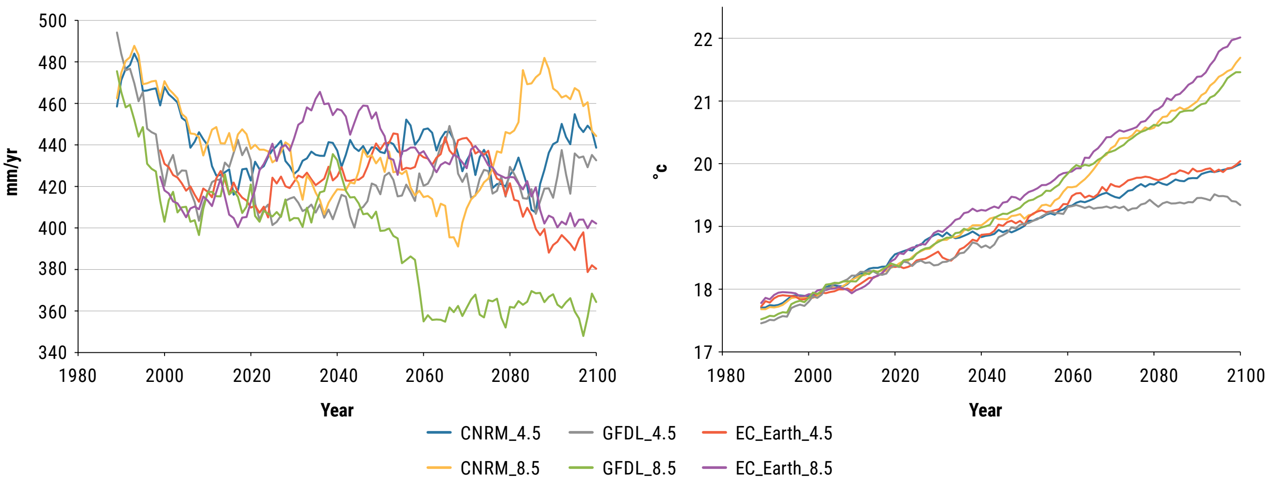

Wadi Diqah River Basin

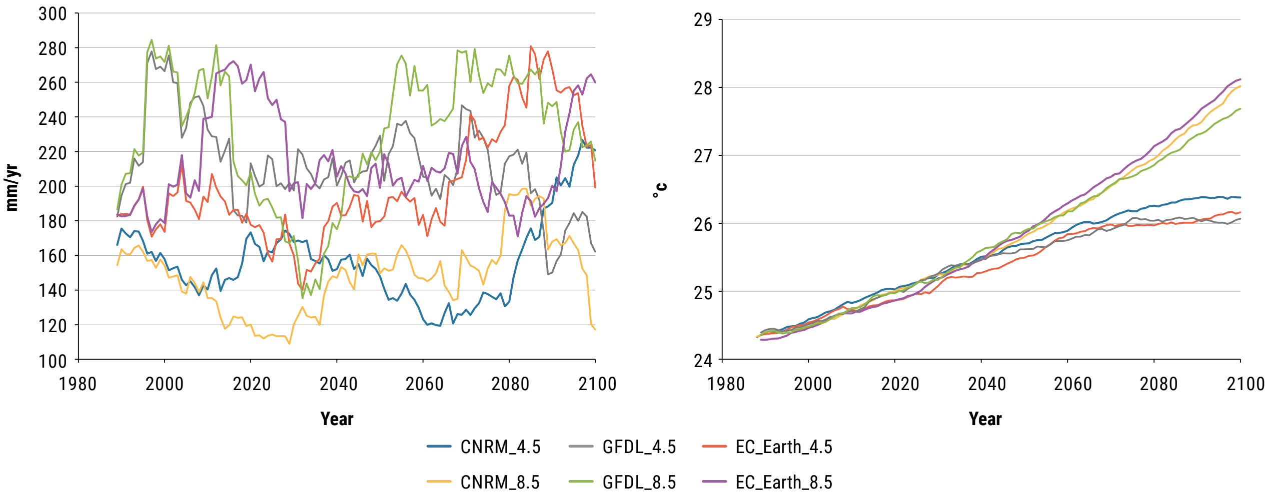

Medjerda River Basin

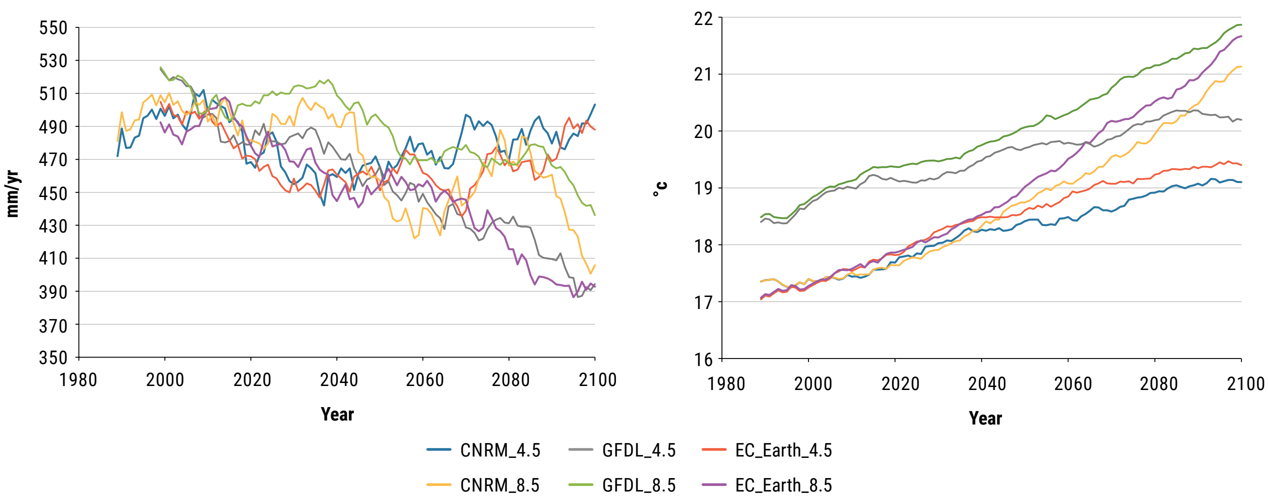

2.2 Observed rainfall and discharge data

2.2.1 Nahr el Kabir River Basin

Rainfall data for the Nahr el Kabir River basin was collected from three stations (Figure 6). Time series for daily discharge data were collected from the two stations located on the main river course as seen in Figure 7.

FIGURE 6: Rainfall stations in the Nahr El Kabir River basin

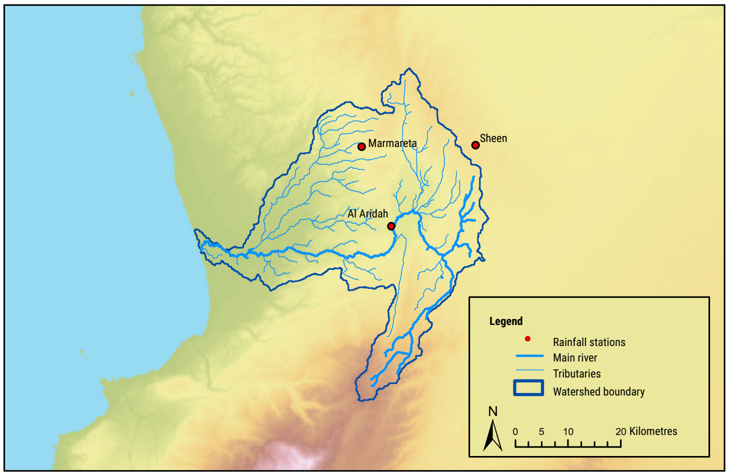

Station Name	Longitude (degree)	Latitude (degree)	Average rainfall (mm)	Period of available data
Al Aridah	36.30139	34.66881	820	1958-2002
Marmareta	36.24982	34.78307	1080	1980-2005
Sheen	36.44257	34.78419	1053	1985-2007

FIGURE 7: Hydrometric stations in the Nahr El Kabir River basin

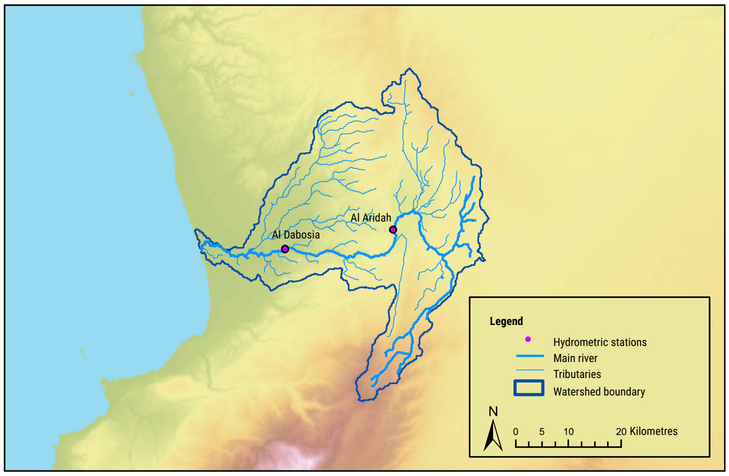

Station Name	Longitude (degree)	Latitude (degree)	Average rainfall (mm)	Period of available data
Aridah	36.30306	34.66514	1955-2007	1958-2002
Al Dabosia	36.11917	34.63883	1989-2007	1980-2005

2.2.2 Wadi Diqah River Basin

Available rainfall and streamflow data were collected from different stations in the basin. Six stations were selected for daily rainfall time series (Figure 8) and four stations located on the main river course were considered for daily discharge time series (Figure 9).

FIGURE 8: Rainfall stations in the Wadi Diqah River basin

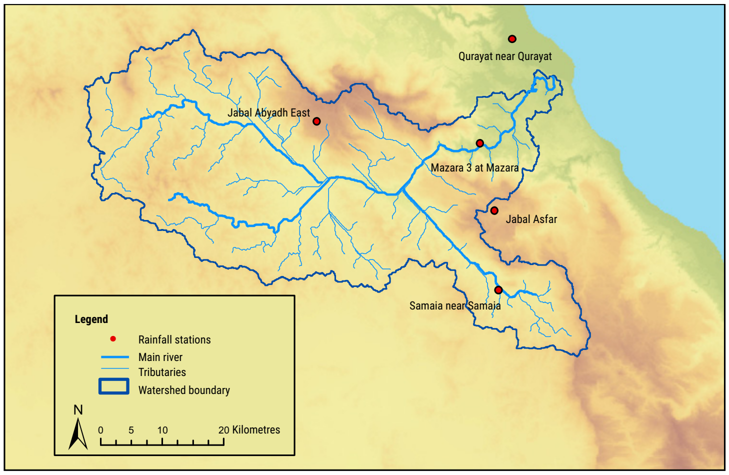

Station Name	Longitude (degree)	Latitude (degree)	Period of available data
Jabal Abyadh East	58.61916	23.12159	1998-2010
Samaia near Samaia	58.88351	22.89381	2007-2010
Jabal Asfar	58.87817	23.00133	1994-2010
Mazara 3 at Mazara	58.85698	23.09188	1977-2010
Qurayat near Qurayat	58.90386	23.23219	1987-2010
Jabal at Tayyin 2	58.32238	23.32576	1995-2010

FIGURE 9: Hydrometric stations in the Wadi Diqah River basin

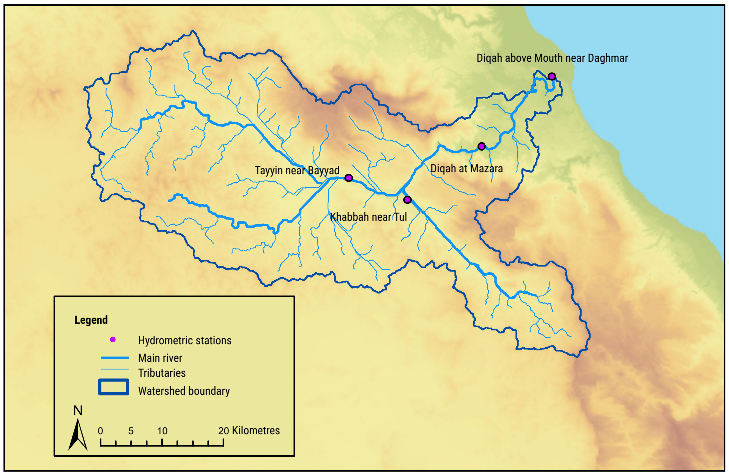

Station Name	Longitude (degree)	Latitude (degree)	Period of available data
Tayyin near Bayyad	58.66607	23.04615	1983-2009
Diqah at Mazara	58.85987	23.08914	1978-2007
Khabbah near Tul	58.75156	23.01633	1992-2008
Diqah above Mouth near Daghmar	58.96177	23.18270	1992-2010

2.2.3 Medjerda River Basin

Four stations were used within the Medjerda River basin to collect rainfall data (Figure 10). Daily discharge data was collected from the three stations located on the main river course displayed in Figure 11.

FIGURE 10: Rainfall stations in the Medjerda River basin

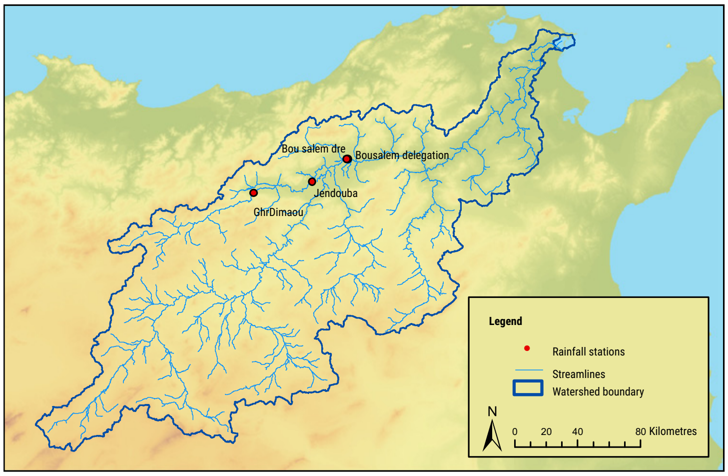

Station Name	Longitude (degree)	Latitude (degree)	Period of available data
Bousalem delegation	36.6075	8.971111	1971-2005
Bou salem dre	36.60833	8.965834	1964-2005
GhrDimaou	36.45115	8.43431	1951-2005
Jendouba	36.50422	8.76841	1900-2005

FIGURE 11: Hydrometric stations in the Medjerda River basin

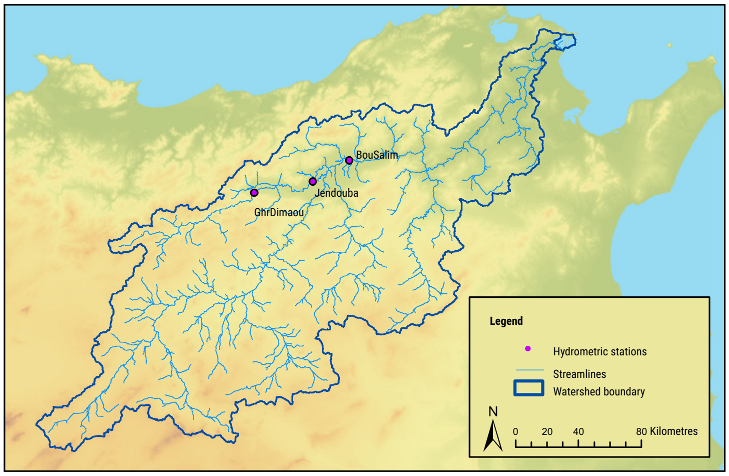

Station Name	Longitude (degree)	Latitude (degree)	Period of available data
BouSalim	36.60106	8.97601	1954-2000
GhrDimaou	36.45115	8.43431	1950-2000
Jendouba	36.50422	8.76841	1900-2000

3 METHODOLOGY

3.1 Extreme temperature and precipitation

Projected trends in extreme temperature and precipitation indices were studied for each of the three basins.

A set of indices for climate extremes were developed by the WMO Expert Team on Climate Change Detection and Indices (ETCCDI) with the aim of providing an easily understandable and manageable set of indices for impact studies and to make multi-model comparisons possible. The set comprises a total of 27 temperature or precipitation-related indices which are commonly calculated based on daily observed precipitation data and daily minimum and maximum temperatures.[6]

The present case study analyses 8 indicators from the ETCCDI list and two additional region-specific variables that were considered more relevant for the Arab region, namely summer days over 35 °C (SU35) and summer days over 40 °C (SU40). The variables studied are presented in Table 2.

TABLE 2: Extreme temperature and precipitation indicators studied

Indicator	Definition	unit
Extreme temperatures		
WSDI (Warm Spell Duration Index)	Annual number of days with at least 6 consecutive days when Tmax>90th percentile	No. of days/yr
CSDI (Cold Spell Duration Index)	Annual number of days with at least 6 consecutive days when Tmin <10th per centile	No. of days/yr
TR (tropical nights)	Annual number of days when daily minimum temperature > 20°C	No. of days/yr
SU35 (hot days)	Annual number of days when daily maximum temperature > 35°C	No. of days/yr
SU40 (very hot days)	Annual number of days when daily maximum temperature > 40°C	No. of days/yr
Extreme Precipitation		
CDD (maximum length of dry spell)	Maximum number of consecutive days when daily precipitation < 1mm	No. of days/yr
CWD (maximum length of wet spell)	Maximum number of consecutive days when daily precipitation ≥ 1mm	No. of days/yr
R10 (10 mm precipitation days)	Annual number of days when daily precipitation ≥ 10mm	No. of days/yr
R20 (20 mm precipitation days)	Annual number of days when daily precipitation ≥ 20mm	No. of days/yr
SDII (Simple Daily Intensity Index)	The ratio of annual total precipitation to the number of wet days (≥ 1mm)	mm/day

Source: based on ETCCDI, 2009.

The methodology to assess the trends in extreme events consisted the following steps:

1. Extraction of RCM daily temperature data (Tmax; Tmin) and precipitation projections generated under RICCAR until the end of the century and for both emission scenarios RCP 4.5 and RCP 8.5.
2. Performing a quality control run of daily Tmax, Tmin and precipitation time series for inhomogeneities using the RClimDex package developed by Zhang and Yang, 2004.[7] Daily maximum and minimum temperature records were defined as outliers if they were outside the range of six standard deviations from the mean of the records (Mean ± 6 × STDEV).
3. Processing of datasets into indices of climate extremes using the RClimDex package.
4. Analysis of results to detect projected changes in extreme indices over time.

3.2 Drought events

Projected changes in drought events in the three basins were analysed using precipitation projection datasets generated under RICCAR for both emission scenarios until the end of the century.

The drought assessment was based on the Standardized Precipitation Index (SPI) according to the method developed by McKee et al.,1993, which measures drought based on the degree to which precipitation in a given time period diverges from the historical median.[8] An SPI of zero indicates that rainfall is at the median value.

SPI indices are timescale-specific and compare precipitation totals for a specific period over all previous years of available data for the same period. Different timescales can be considered, namely three, six, 12, 24, and 48 months. Two timescales were selected for this study. The first is the six-month SPI (November–end of April for Nahr el Kabir and Medjerda rivers; May–end of October for Wadi Diqah), which is also referred to as agricultural drought and gives an important indication of rainfall patterns during the agricultural season in the basins. The other timescale considered is the 12-month SPI (starting November) or hydrological drought, which reflects long-term precipitation.

As defined by McKee et al.,1993, SPI values are classified into different drought categories with SPI < −1.0 indicating a moderate drought, SPI < −1.5 a severe drought, and SPI < −2.0 reflecting an extreme drought.

The approach applied to estimate drought events was based on the following steps:

1) Extraction of RCM precipitation projections generated under RICCAR until the end of the century and for both emission scenarios RCP 4.5 and RCP 8.5. The ArcGIS software was used to extract precipitation time series from NetCDF files.

2) Calculation of drought indices based on precipitation time series according to the different SPI selected timescales.

3) Analysis of results to detect projected changes in drought events over time.

The SPI values were calculated according to a gamma distribution using Microsoft Excel according to the computation presented herein.

For the chosen timescale (six-month and 12- month) a lagged moving average was computed for the monthly precipitation time series, hence the value at month *i* also accounts for conditions in the preceding *i*–1 months. The SPI value was then computed by fitting a probability density function to a given precipitation summed over the time scale of interest. The monthly precipitation was fitted to a gamma distribution, with the probability density function defined as:

$$g(x)\,\frac{1}{\beta^{a}\,T(\alpha)}\,x^{\alpha-1}e^{-x/\beta} = for\ x > 0$$

Where, x>0, x is the precipitation amount, α is a shape parameter, β>0, β is the scale parameter

$\tau(a) = \int_0^\infty y^{\alpha-1}e^{-y}dy\ \tau(a)$ is the gamma function

Fitting the distribution to the data requires α and β to be estimated. The maximum likelihood function is given as follows:

$$\widehat{\alpha} = \frac{1}{4\,A}\left[1 + \sqrt{1 + \frac{4A}{3}}\right]$$

$$\widehat{\beta} = \frac{\overline{x}}{\widehat{\alpha}} \quad \text{where} \quad A = 1n(\overline{x}) - \frac{\sum 1n(x)}{n}$$

Where n is the number of precipitation observations

The resulting parameters were then used to find the cumulative probability of an observed precipitation event for the given month and time scale for the station of concern. The cumulative probability is given by:

$$G(x) = \int_0^x g(x)dx = \frac{1}{\beta\alpha\tau(\widehat{\alpha})}\int_o^x x^{\widehat{\alpha}-1}\,e^{-x/\widehat{\beta}}\,dx$$

Letting $t = x/\widehat{\beta}$

The equation becomes:

$$G(x) = \frac{1}{\tau(\widehat{\alpha})}\int_o^x t^{\widehat{\alpha}-1}e^{-t}dt$$

Since the gamma function is undefined for x=0 and precipitation distribution may contain zero, cumulative probability becomes:

$$H(x) = q + (1-q)\, G(x)$$

where q is the probability of zero.

H(x) is then transformed to a normal distribution with a zero mean and unit variance.

The above approach is simple but not practical for computing SPI for large numbers of data points.

As used by Edwards and McKee (1997), the approximate conversion provided by Abramowitz and Stegun (1965) is an alternative and was used in this study as follows:

$$SPI = -\left[t - \frac{C_0 + C_1^t + C_2^{t^2}}{1 + d_1^t + d_2^{t^2} + d_3^{t^3}} \right] \qquad \text{for } 0<H(x)<0$$

$$Z = SPI = \left[t - \frac{C_0 + C_1^t + C_2^{t^2}}{1 + d_1^t + d_2^{t^2} + d_3^{t^3}} \right] \qquad \text{for } 0.5<H(x)<1.0$$

$$\text{Where } t = \sqrt{1n\left[\frac{1}{(H(x))^2}\right]} \qquad \text{for } 0<H(x)<0.5$$

$$\sqrt{1n\left[\frac{1}{(1.0-H(x))^2}\right]} \qquad \text{for } 0.5<H(x)<1.0$$

C_0=2.515517 , C_1=0.802853, C_2=010328

d_1= 1.432788, d_2=0.189269 , d_3=0.001

It is important to note that the α and β parameters of the γ probability density function were computed for the reference period (1986–2005) then were fixed when SPI was calculated for projected climate data (2006–2100).

3.3 Extreme flood events

The assessment of the impact of climate change on extreme flow was carried out using the Hydrologic Engineering Center Hydrological Modelling System (HEC-HMS) model and the Arc GIS extension HEC-GeoHMS.[9] This model was developed by the Hydrologic Engineering Centre (HEC) of the United States Army Corps of Engineers and is a GIS-based semi-distributed rainfall-runoff model. It is used for used for computing the flow direction, flow accumulation, stream delineation, watershed delineation and drainage networks derivation. Additional possible simulated processes include canopy and surface processes, snow accumulation and melting, as well as soil and groundwater processes. The basin model within HEC-HMS handles infiltration loss and base flow computations in addition to the rainfall runoff transformation process.

The Soil Moisture Accounting (SMA) method was selected within HEC-HMS for this analysis, as it allows for a long-term continuous simulation of hydrologic processes. The meteorological model within HEC-HMS is the major component responsible for defining the meteorological boundary conditions for the basins. It includes precipitation, evapotranspiration and snowmelt method control specifications and input data (time series, paired data and gridded data).

The different steps followed to assess changes in extreme flow events consisted of the following:

1) Collection of observed climate and river discharge data for at least two stations in each of the selected basins, as well as topographic, land use and soil data pertaining to each basin.

2) Extraction of RCM daily precipitation and temperature projections generated under RICCAR until the end of the century and for both emission scenarios RCP 4.5 and RCP 8.5.

3) Calibration and validation of the HEC-HMS model for the three selected river basins.
River discharge data was used for model calibration and validation. The following parameters were identified to be sensitive parameters: soil maximum infiltration rate, soil percolation, and groundwater water percolation. A combination of a visual assessment and the univariate gradient method were used to achieve optimal calibration in order to minimize differences between observed versus modelled annual flow volume.

4) Performing hydrological simulations for the reference period and for future periods under different emission scenarios. Downscaled RCM daily temperature and precipitation projections generated under RICCAR over the Arab Domain were used as inputs to the hydrological model as the climate data for different time periods and emission scenarios. Potential evapotranspiration was also used as an input and computed within the HEC-HMS model using the Priestley-Taylor method. Hydrological model runs were then performed separately on individual RCM ensemble member simulations (RCA4_EC EARTH, RCA4_CNRM-CM5, and RCA4_GFDL-ESM) covering the period 1970–-2100 for RCP 4.5 and RCP 8.5. A total of six runs were thus applied for each basin. For each RCP, the ensemble mean streamflow value from the three model runs was then calculated and used as a result for the analysis (Figure 12).

FIGURE 12: Hydrological simulations

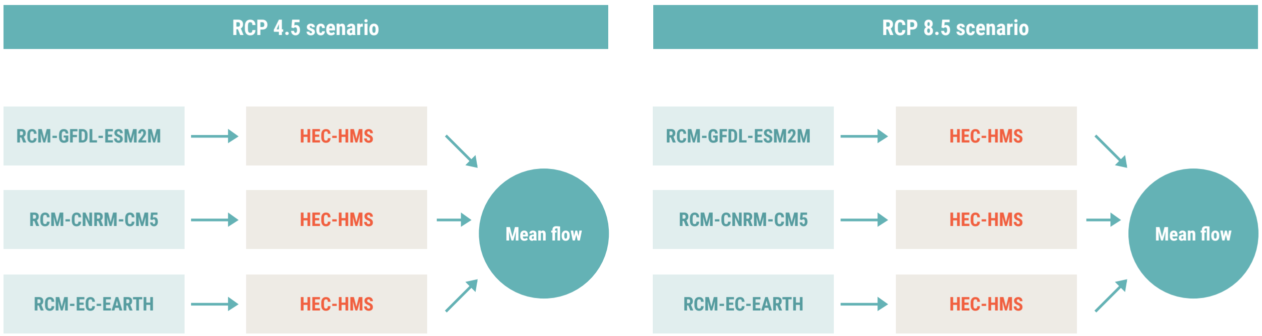

5) Based on the outputs, two sets of analyses were used to detect projected changes in the frequency and magnitude of extreme streamflow events until the end of the century in the selected basins (Table 3). The first aimed at identifying changes in the frequency of extreme peak flow discharges, which represent flow events exceeding the 90th percentile values of the maximum daily streamflow value. The second analysis investigated changes in the 100-year flood value, which refers to extreme flow events with return periods equal to, or larger than, 100 years. The Gumbel frequency distribution was used for flood-frequency analyses, and the variables were estimated using the maximum likelihood method.

TABLE 3: Extreme flood indicators studied

Indicator	Definition	unit
90^{th} percentile high flow days	number of days exceeding the 90th percentile values of the maximum daily streamflow value	No. of days
100-yr flood value	flow value of extreme flow events with return periods equal to, or larger than, 100 years	m^3/s

4 RESULTS

4.1 Nahr el Kabir River Basin

4.1.1 Extreme temperature and precipitation

All temperature indicators indicate trends towards drier conditions in the basin, apparent from projected increases in warm temperature indicators and decreases in cold spells (Table 4 and Figure 13). For instance, SU35 is projected to increase from 60 days to 88 and 98 days at mid- and end-century, respectively, for RCP 4.5 and up to 93 and 124 days for RCP 8.5 (Table 4). The trend of increased temperature indicators is more pronounced under RCP 8.5. In general, for both emission scenarios, projections for all extreme temperature indices show significant differences at the mid and the end of the century in comparison to the reference period using the Student's t-test at $p < 0.05$ as seen in Table 4.

As for precipitation indicators, results are variable. For instance, there is a significant amount of variability for the CDD indicator with no obvious temporal pattern: for RCP 4.5, mean values show an increase by three days at mid-century, followed by a decrease of three days at end-century compared to the reference period. A rise in CDD trends is shown during the mid-century period (Figure 13). On the other hand, less heavy rain (R10) is projected over time, even though very heavy rain (R20) is projected to increase. Increases in rain intensity are projected for both scenarios over time as exhibited by the changes in the SDII indicator. Using the Student's t-test at $p < 0.05$, results for most of the investigated extreme precipitation indices for both emission scenarios exhibit significant differences at the mid and end of the century in comparison to the reference period (Table 4).

TABLE 4: Extreme event indices mean values for different emission scenarios and time periods for Nahr el Kabir River basin

Index	Emission scenario	1986-2005	2046-2065	2081-2100
Extreme temperature indices				
WSDI (days/yr)	RCP 4.5	10 a	32 b	44 c
	RCP 8.5		44 b	94 c
CSDI (days/yr)	RCP 4.5	5.5 a	1.9 b	1.3 c
	RCP 8.5		0.5 b	0.2 c
TR (days/yr)	RCP 4.5	52 a	81 b	93 c
	RCP 8.5		89 b	119 c
SU35 (days/yr)	RCP 4.5	60 a	88 b	98 c
	RCP 8.5		93 b	124 b
SU40 (days/yr)	RCP 4.5	5 a	15 b	18 c
	RCP 8.5		16 b	36 c
Extreme precipitation indices				
CDD (days/yr)	RCP 4.5	113 a	116 a	110 b
	RCP 8.5		113 a	112 b
CWD (days/yr)	RCP 4.5	7.1 a	7.0 b	6.9 b
	RCP 8.5		6.9 b	6.6 c
R10mm (days/yr)	RCP 4.5	13 a	12.9 b	12.3 b
	RCP 8.5		12 b	12.1 c
R20mm (days/yr)	RCP 4.5	2.6 a	3 b	2.9 c
	RCP 8.5		2.7 b	3.1 c
SDII (mm/day)	RCP 4.5	5.8 a	6 b	5.9 a
	RCP 8.5		5.9 b	6.1 c

Means followed by different letters indicate statistically significant differences according to the Student's t-test ($p < 0.05$)

FIGURE 13: Mean change in selected extreme events indices over time for ensemble of three RCP 4.5 and RCP 8.5 projections for the Nahr el Kabir River basin

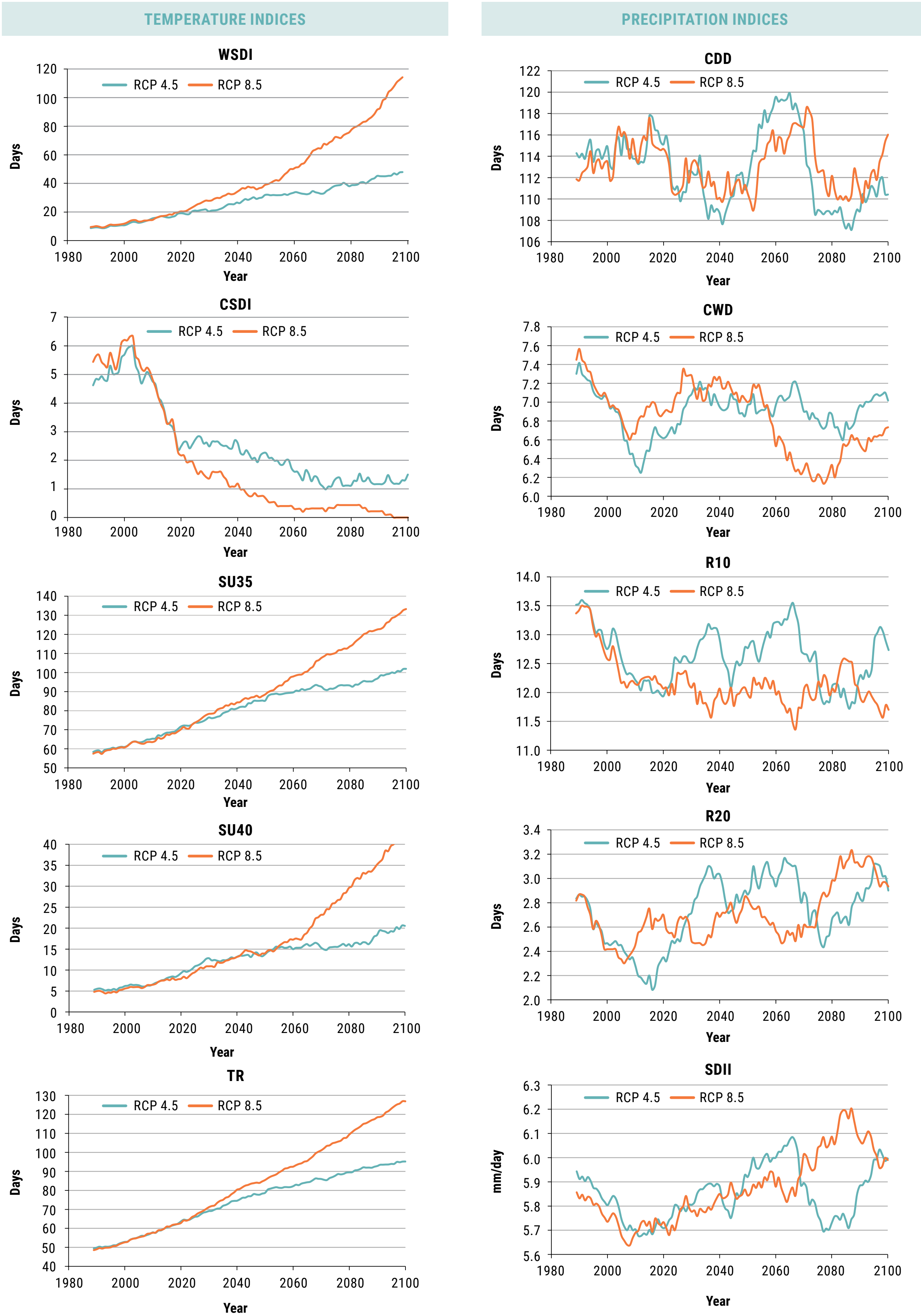

4.1.2 Drought events

Projected SPI trends time series over time are presented in Figure 14 and Figure 15 for the six-month and the 12-month, respectively.

When evaluating the six-month SPI (Table 5), results show that moderate drought occurs 55% of the time (percentage in terms of months) for the reference time period. For RCP 4.5, it changes to 45% and 65% of the time at mid- and end-century, respectively, and becomes more intense for RCP 8.5 with moderate drought occurring 75% and 90% of the time at mid and end-century, respectively. However, the Student's t-test at $p < 0.05$ showed that the changes in the six-month SPI were not significant at mid and end-century in comparison to the reference period for both emission scenarios.

When evaluating the 12-month SPI, results show that moderate drought occurs 60% of the time for the reference period and is projected at 55% for mid-century and 65% at end-century for RCP 4.5 as shown in Table 5. A strong increase is projected at RCP 8.5, with occurrences of 75% and 80% at mid- and end-century, respectively. The Student's t-test at $p < 0.05$ has indicated that changes in the 12-month SPI were significant only for RCP 8.5 at end-century in comparison to the reference period and to mid-century.

In summary, when comparing future projections, results show that a strong increase in the percentage of time with moderate drought conditions is expected towards end-century. There are no projected severe or extreme droughts in the six- or 12-month SPI in the basin.

FIGURE 14: Projected six-month SPI trends over time for ensemble of three RCP 4.5 and RCP 8.5 projections for the Nahr el Kabir River basin

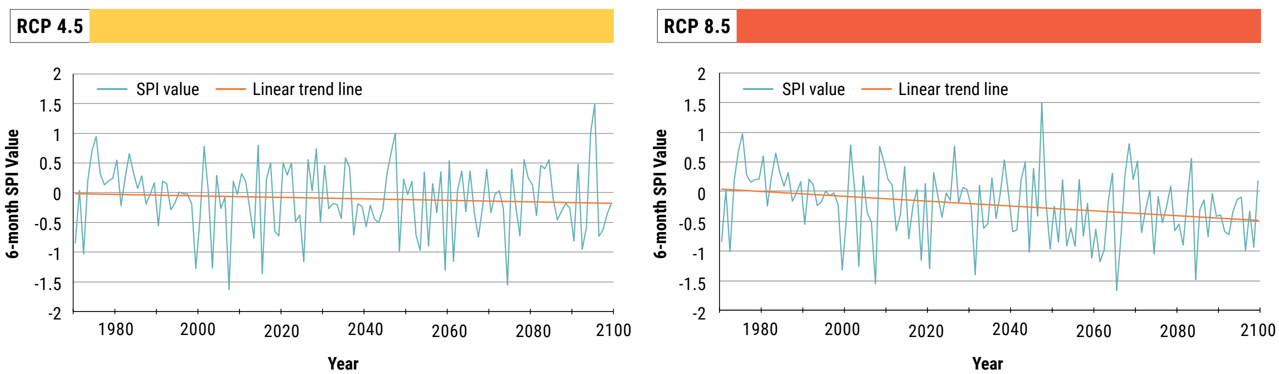

FIGURE 15: Projected 12-month SPI trends over time for ensemble of three RCP 4.5 and RCP 8.5 projections for the Nahr el Kabir River basin

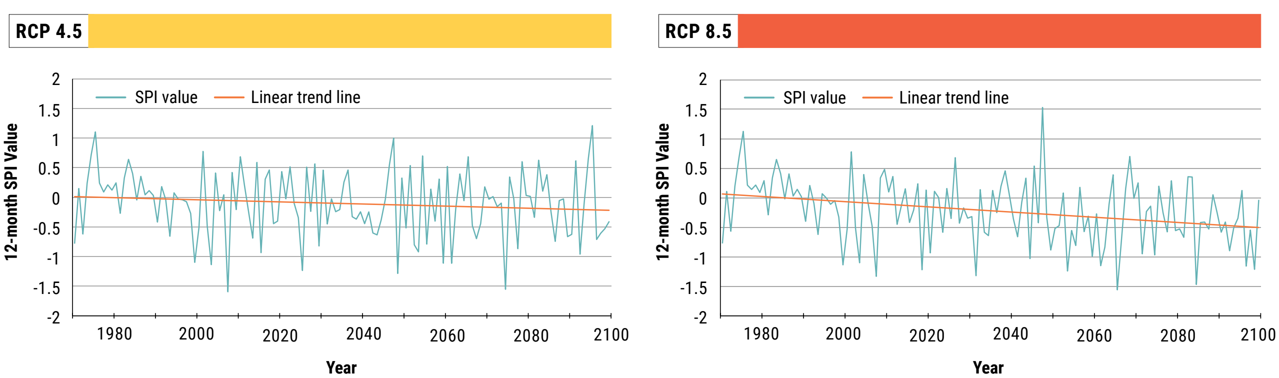

TABLE 5: Projected percentage of time with moderate, severe and extreme drought conditions until the end of the century for the six-month SPI value and the 12-month SPI value in the Nahr el Kabir River basin

Drought conditions	Drought occurrence (%)				
	Reference period (1986-2005)	Mid-century (2046-2065)		End-century (2081-2100)	
		RCP 4.5	RCP 8.5	RCP 4.5	RCP 8.5
Six-month SPI value					
Moderate (SPI < −1.0)	55	45	75	65	90
Severe (SPI < −1.5)	0	0	0	0	0
Extreme (SPI < −2.0)	0	0	0	0	0
TOTAL	**55**	**45**	**75**	**65**	**90**
12-month SPI value					
Moderate (SPI < −1.0)	60	55	75	65	80
Severe (SPI < −1.5)	0	0	0	0	0
Extreme (SPI < −2.0)	0	0	0	0	0
TOTAL	**60**	**55**	**75**	**65**	**80**

4.1.3 Extreme flood events

Results show that the 90th percentile high flow days are projected to increase for both emissions scenarios in this basin (Figure 16). Moreover, trends for the 100-year flood values are projected to significantly rise for both emission scenarios. Results for RCP 8.5 show changes in value from 126 m^3/s at the reference period to 131 m^3/s and 149 m^3/s at mid- and end-century, respectively (Figure 17 and Table 6).

FIGURE 16: Mean number of 90th percentile high-flow days for different emission scenarios and time periods for the Nahr el Kabir River basin

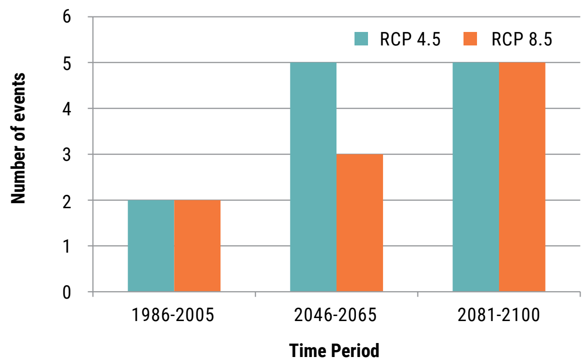

FIGURE 17: Mean change in the 100-year flood value (m^3/s) over time for ensemble of three RCP 4.5 and RCP 8.5 projections for the Nahr el Kabir River basin

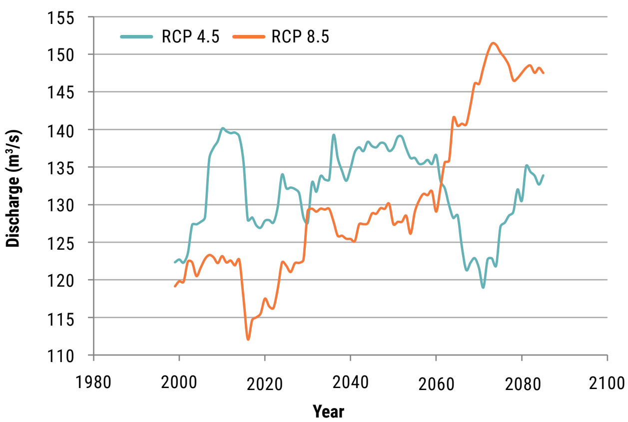

TABLE 6: Mean ensemble 100-year flood values (m^3/s) for different emission scenarios and time periods for the Nahr el Kabir River basin

Emission scenario	1986–2005	2046–2065	2081–2100
RCP 4.5	126 a	136 b	128 c
RCP 8.5		131 b	149 c

Means followed by different letters indicate statistically significant differences according to the Student's t-test ($p < 0.05$)

4.2 Wadi Diqah River Basin

4.2.1 Extreme temperature and precipitation

Results for extreme temperature and precipitation for the Wadi Diqah River basin are presented in Table 7 and Figure 18.

All temperature indicators show a trend towards drier conditions in the Wadi Diqah basin. SU35 is projected to increase from 40 days in the reference period to 77 days and 89 days at mid- and end-century, respectively for scenario RCP 4.5. The trends for RCP 8.5 are more pronounced with increases to 88 days and 130 days, respectively, at mid- and end-century. In general, for both emission scenarios, all extreme temperature indices exhibited significant differences at mid and end-century in comparison to the reference period using the Student's t-test at $p < 0.05$ (Table 7).

Projections for precipitation indicators indicated a clear increasing trend for CDD in concordance with slight decreasing trends in CWD. On the other hand, both R10 and R20 show increases towards the end of the century and projected changes in SDII indicate that more intense precipitation events are projected for both emission scenarios. Using the Student's t-test at $p < 0.05$, results have indicated that for both RCP 4.5 and RCP 8.5, most of the investigated extreme precipitation indices show significant differences at both future periods in comparison to the reference period (Table 7).

TABLE 7: Extreme event indices mean values for different emission scenarios and time periods for the Wadi Diqah River basin

Index	Emission scenario	1986-2005	2046-2065	2081-2100
Extreme temperature indices				
WSDI (days/yr)	RCP 4.5	12 a	93 b	130 c
	RCP 8.5		117 b	236 c
CSDI (days/yr)	RCP 4.5	1.3 a	0.3 b	0.2 c
	RCP 8.5		0.1 b	0 c
TR (days/yr)	RCP 4.5	187 a	207 b	213 c
	RCP 8.5		212 b	238 c
SU35 (days/yr)	RCP 4.5	40 a	77 b	89 c
	RCP 8.5		88 b	130 c
SU40 (days/yr)	RCP 4.5	0 a	0.5 b	1.9 c
	RCP 8.5		1.8 b	16.8 c
Extreme precipitation indices				
CDD (days/yr)	RCP 4.5	115 a	128 b	126 b
	RCP 8.5		124 b	139 c
CWD (days/yr)	RCP 4.5	4.1 a	4.2 b	4.0 c
	RCP 8.5		4.0 b	4.1 b
R10mm (days/yr)	RCP 4.5	4.3 a	4.0 a	4.4 a
	RCP 8.5		4.5 ab	4.5 b
R20 mm (days/yr)	RCP 4.5	2.1 a	2.0 b	2.3 c
	RCP 8.5		2.2 b	2.4 c
SDII (mm/day)	RCP 4.5	9.1 a	9.2 a	10.6 b
	RCP 8.5		10.6 b	11.4 c

Means followed by different letters indicate statistically significant differences according to the Student's t-test ($p < 0.05$)

FIGURE 18: Mean change in selected extreme events indices over time for ensemble of three RCP 4.5 and RCP 8.5 projections for the Wadi Diqah River basin

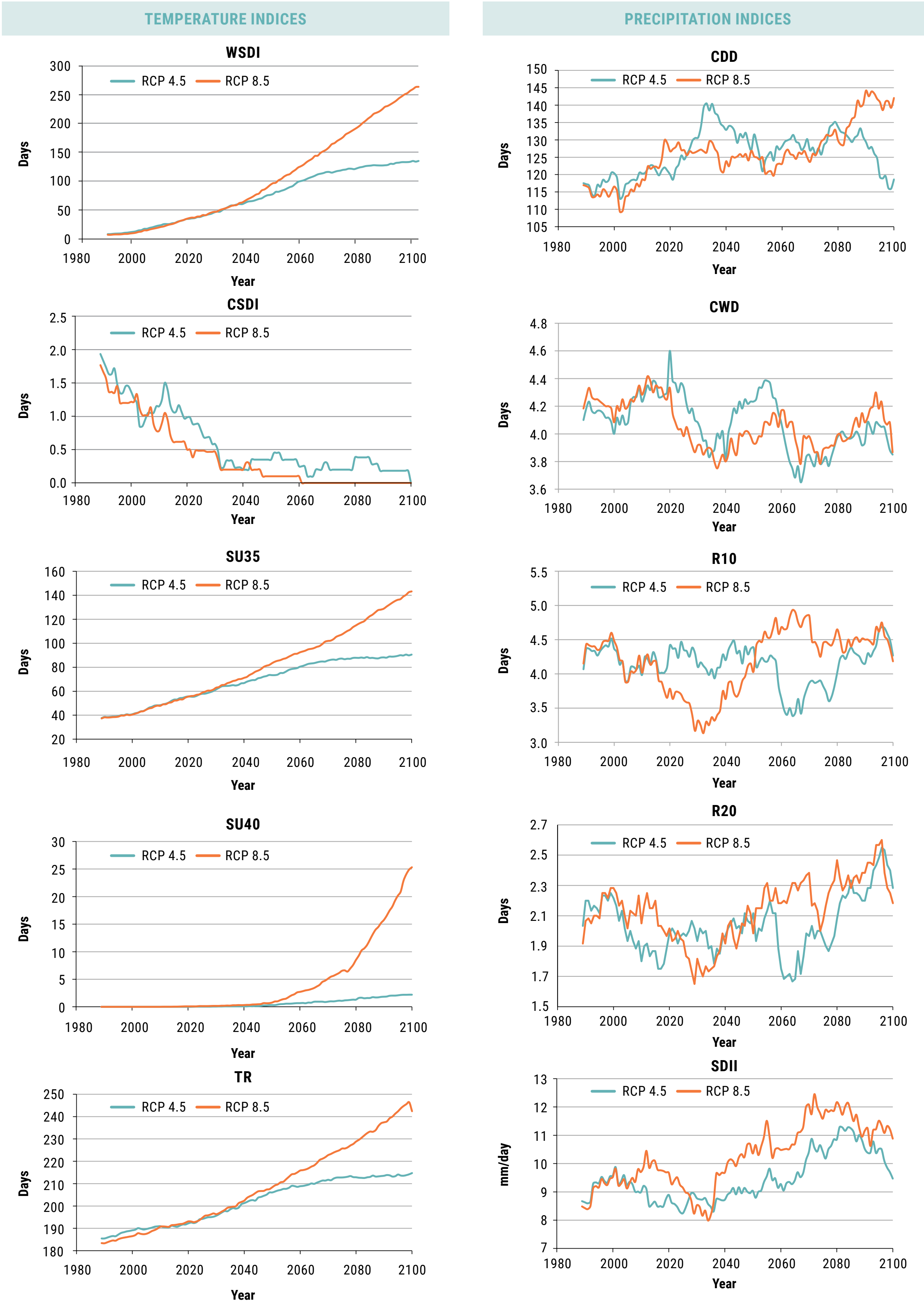

4.2.2 Drought events

As shown in Figure 19 and Figure 20, a positive trend for SPI values is projected for both emission scenarios over the years, though this change in trend is not significant according to the Mann-Kendall test (α=0.05). Evaluation of results in terms of percentage of occurrence shows an overall decrease in the occurrence of moderate drought for the six-month SPI (Table 8). For RCP 4.5, values for the six-month SPI vary from 60% of the time in the reference period to 50% both at mid- and end-century for RCP 4.5. For RCP 8.5, a decrease in total drought occurrence compared to the reference period is projected at end-century with a 40% occurrence.

As for the 12-month SPI, a slight overall increase in moderate drought occurrence is projected for RCP 4.5 compared to the reference period which exhibits an occurrence of 55% (values of 65% and 60% for mid- and end-century, respectively). For RCP 8.5, there is no apparent marked change in moderate drought occurrence in comparison to the reference period at mid-century. No severe or extreme droughts are detected in this basin.

Using the Student’s t-test at $p < 0.05$, results have shown that for both emission scenarios, changes in the six-month and 12-month SPI were not significant.

FIGURE 19: Projected six-month SPI trends over time for ensemble of three RCP 4.5 and RCP 8.5 projections for the Wadi Diqah River basin

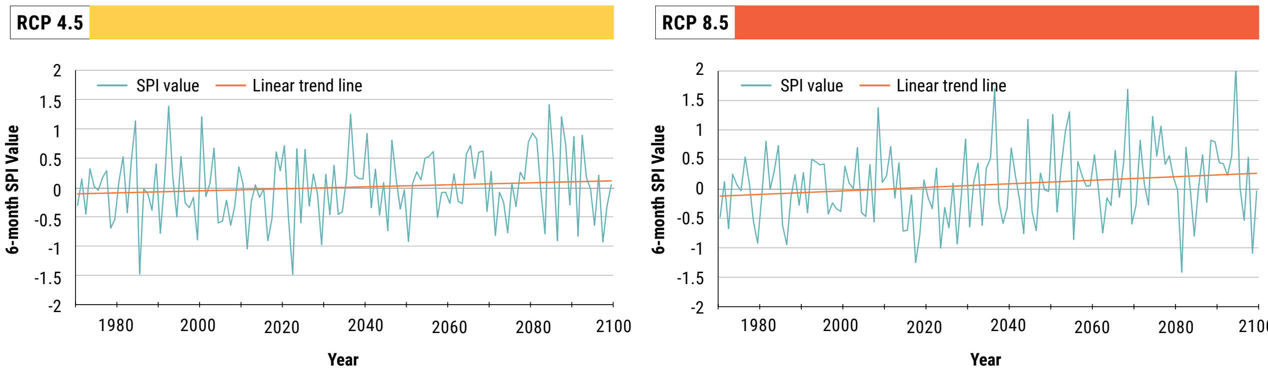

FIGURE 20: Projected 12-month SPI trends over time for ensemble of three RCP 4.5 and RCP 8.5 projections for the Wadi Diqah River basin

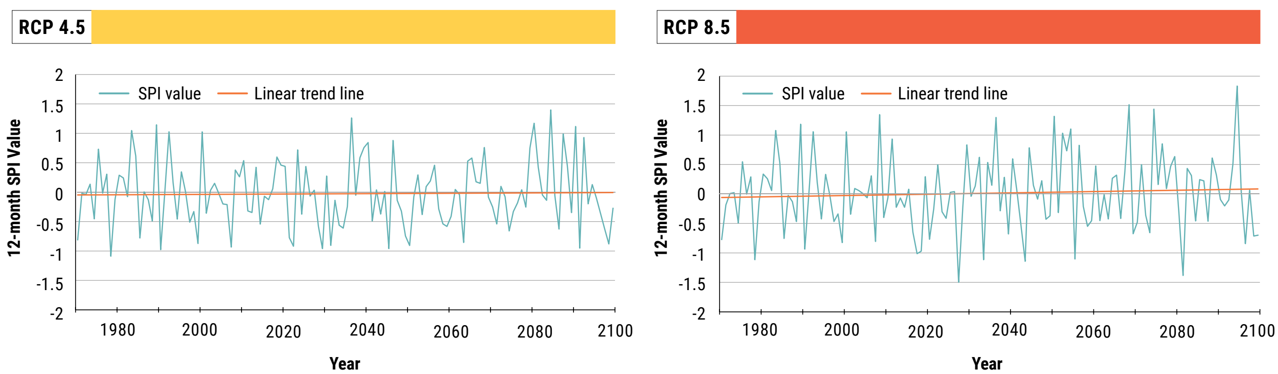

TABLE 8: Projected percentage of time with moderate, severe and extreme drought conditions until the end of the century for the six-month SPI value and the 12-month SPI value in the Wadi Diqah River basin

Drought conditions	Drought occurrence (%)				
	Reference period (1986-2005)	Mid-century (2046-2065)		End-century (2081-2100)	
		RCP 4.5	RCP 8.5	RCP 4.5	RCP 8.5
Six-month SPI value					
Moderate (SPI < −1.0)	60	50	50	50	40
Severe (SPI < −1.5)	0	0	0	0	0
Extreme (SPI < −2.0)	0	0	0	0	0
TOTAL	**60**	**50**	**50**	**50**	**40**
12-month SPI value					
Moderate (SPI < −1.0)	55	65	55	60	50
Severe (SPI < −1.5)	0	0	0	0	0
Extreme (SPI < −2.0)	0	0	0	0	0
TOTAL	**55**	**65**	**55**	**60**	**50**

4.2.3 Extreme flood events

As shown in Figure 21, results for the 90th percentile high flow days for Wadi Diqah reveal a decrease at mid-century compared to the reference period followed by an increase at end-century for both emissions scenarios. The 100-year flood value is projected to rise for both RCPs at the end of the century after a decrease at mid-century (Figure 22). Using Student's t-test at $p < 0.05$, results have indicated that changes for the 100-year flood value were significant except for RCP4.5 at mid-century (Table 9).

FIGURE 21: Mean number of 90th percentile high-flow days for different emission scenarios and time periods for the Wadi Diqah River basin

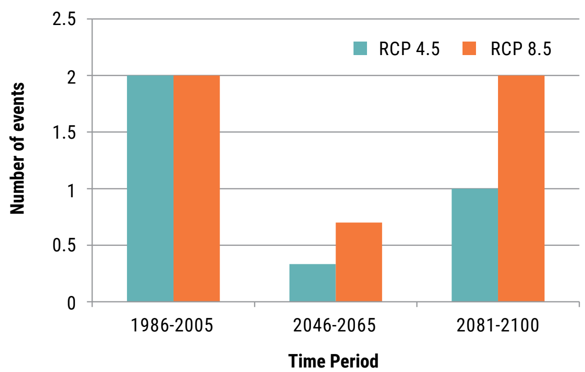

FIGURE 22: Mean change in the 100-year flood value (m^3/s) over time for ensemble of three RCP 4.5 and RCP 8.5 projections for the Wadi Diqah basin

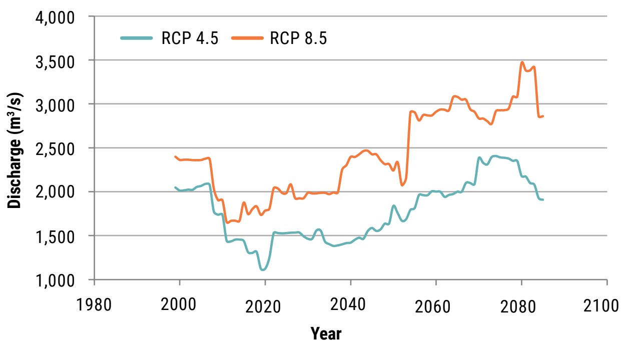

TABLE 9: Mean ensemble 100-year flood values (m^3/s) for different emission scenarios and time periods for the Wadi Diqah River basin

Emission scenario	1986–2005	2046–2065	2081–2100
RCP 4.5	2,150 a	1,836 a	2,275 b
RCP 8.5		2,667 b	3,043 c

Means followed by different letters indicate statistically significant differences according to the Student's t-test ($p < 0.05$)

4.3 Medjerda River Basin

4.3.1 Extreme temperature and precipitation

As shown in Table 15 and Figure 23, changes in extreme temperature indices in the basin indicate consistent trends towards drier conditions, in particular for RCP 8.5. For example, for the emission scenario RCP 4.5, the indicator SU35 is projected to increase from 45 days in the reference period to 65 days and 74 days at mid and end-century, respectively. These change to 71 and 97 days for RCP 8.5. In general, for both emission scenarios, all projections of extreme temperature indices have shown significant differences at mid and end-century in comparison to the reference period using the Student's t-test at $p < 0.05$ (Table 10).

Results for precipitation extremes are more variable. For instance, CDD show decreases throughout mid-century and increases throughout end-century for RCP 8.5 (Figure 23). However, mean CDD values reveal no apparent consistent temporal pattern of change (Table 10). Both R10 and R20 have consistent decreasing trends by the end of the century, while precipitation intensity (SDII) is projected to increase during the end-century period compared to mid-century. Using the Student's t-test at $p < 0.05$, results have shown that for both RCP 4.5 and RCP 8.5, most of the investigated projections of extreme precipitation indices exhibited significant differences at mid and end-century in comparison to the reference period (Table 10).

TABLE 10: Extreme event indices mean values for different emission scenarios and time periods for the Medjerda River basin

Index	Emission scenario	1986-2005	2046-2065	2081-2100
Extreme temperature indices				
WSDI (days/yr)	RCP 4.5	9 a	30 b	40 c
	RCP 8.5		40 b	93 c
CSDI (days/yr)	RCP 4.5	2 a	1.1 b	0.1 c
	RCP 8.5		0.2 b	0.2 c
TR (days/yr)	RCP 4.5	43 a	65 b	75 c
	RCP 8.5		73 b	102 c
SU35 (days/yr)	RCP 4.5	45 a	65 b	74 c
	RCP 8.5		71 b	97 c
SU40 (days/yr)	RCP 4.5	6 a	16 b	21 c
	RCP 8.5		15 b	38 c
Extreme precipitation indices				
CDD (days/yr)	RCP 4.5	35 a	36 b	35 a
	RCP 8.5		35 a	40 b
CWD (days/yr)	RCP 4.5	7.7 a	6.9 b	7.3 c
	RCP 8.5		7.3 a	6.7 b
R10mm (days/yr)	RCP 4.5	10.9 a	9.7 b	9.9 b
	RCP 8.5		9.6 b	9.1 c
R20 mm (days/yr)	RCP 4.5	3.0 a	2.5 b	2.6 b
	RCP 8.5		2.7 b	2.6 b
SDII (mm/day)	RCP 4.5	4.9 a	4.7 b	4.8 a
	RCP 8.5		4.8 b	5.0 c

Means followed by different letters indicate statistically significant differences according to the Student's t-test ($p < 0.05$)

FIGURE 23: Mean change in selected extreme events indices over time for ensemble of three RCP 4.5 and RCP 8.5 projections for the Medjerda River basin

TEMPERATURE INDICES	PRECIPITATION INDICES

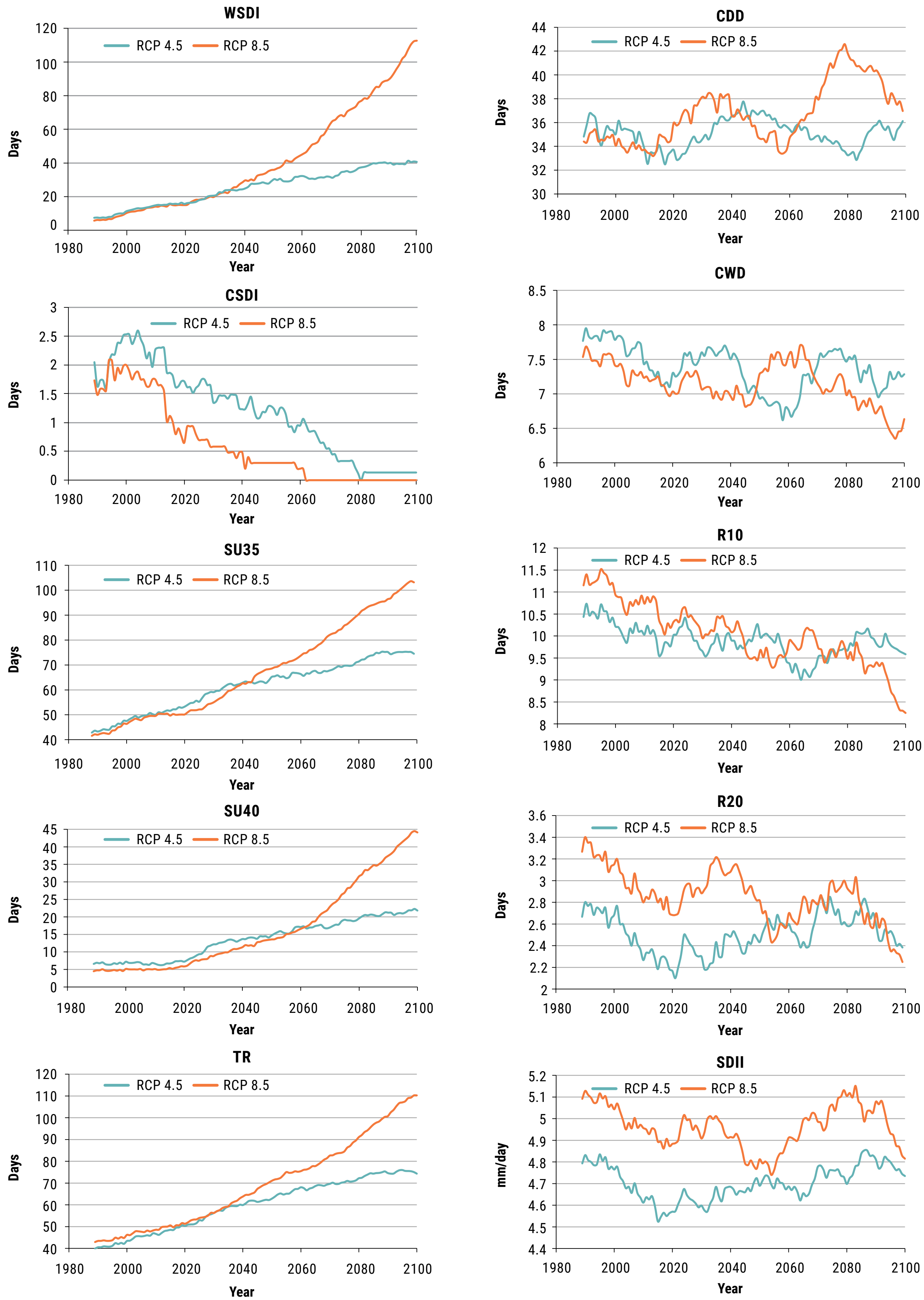

4.3.2 Drought events

Figure 24 and Figure 25 show that SPI values exhibit projected significant negative trends over the years (according to Mann-Kendall test with α=0.05) reflecting a direction towards more extreme drought conditions. Unlike the other basins, the Medjerda River exhibits projected episodes of severe and extreme drought that are not apparent in the reference period, in addition to projected moderate drought for both RCPs over time (Table 11).

Results show an increase in the percentage of time with moderate drought for both SPI time scales and emission scenarios. Furthermore, it can be seen that severe drought conditions are expected to occur much more often by the end of the century, with an occurrence varying between 5% and 25% of the time depending on the SPI scale. As for extreme drought, for the 12-month SPI value, it is projected to occur at the end of the century for the emission scenario RCP 8.5 only (5% occurrence) whereas projections for the six-month SPI show extreme droughts occurring at end-century for both scenarios.

When considering the total of all types of drought conditions, it is projected that drought in the basin will significantly increase for both SPI scales. For instance, the total six-month drought is projected to change from a 60% occurrence in the reference period to a 75% occurrence or more for the future. Similarly, based on the 12-month SPI, drought has the potential to occur up to 95% of the time compared to 50% in the reference period, as seen in Table 11.

FIGURE 24: Projected six-month SPI trends over time for ensemble of three RCP 4.5 and RCP 8.5 projections for the Medjerda River basin

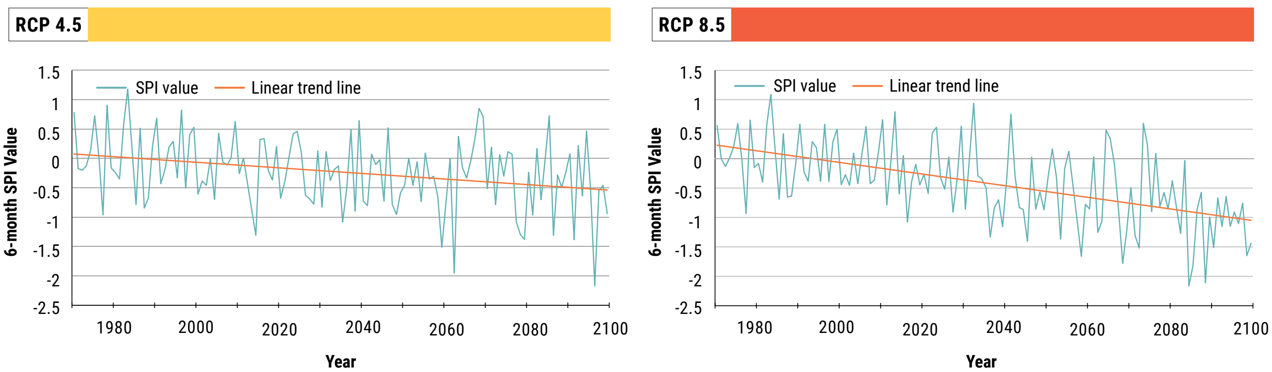

FIGURE 25: Projected 12-month SPI trends over time for ensemble of three RCP 4.5 and RCP 8.5 projections for the Medjerda River basin

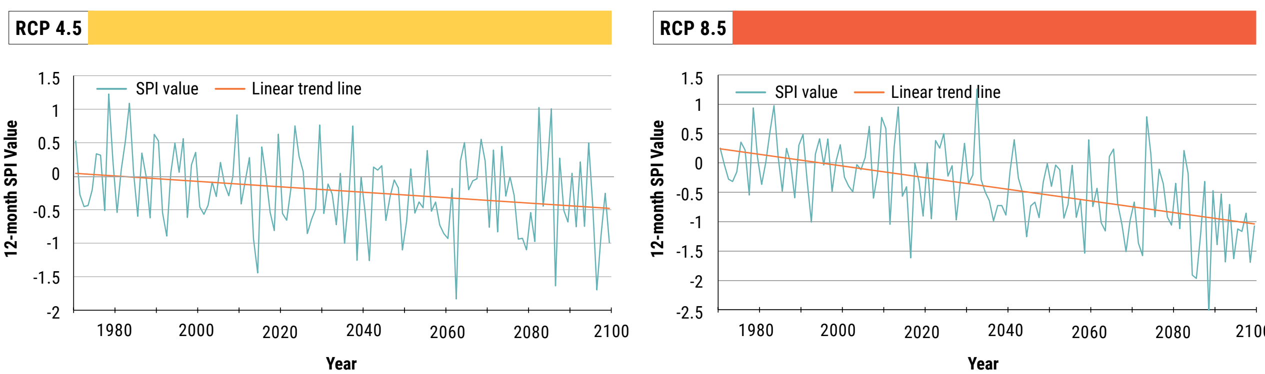

TABLE 11: Projected percentage of time with moderate, severe and extreme drought conditions until the end of the century for the six-month SPI value and the 12-month SPI value in the Medjerda River basin

Drought conditions	Drought occurrence (%)				
	Reference period (1986-2005)	Mid-century (2046-2065)		End-century (2081-2100)	
		RCP 4.5	RCP 8.5	RCP 4.5	RCP 8.5
Six-month SPI value					
Moderate (SPI < −1.0)	60	70	70	70	75
Severe (SPI < −1.5)	0	10	5	0	15
Extreme (SPI < −2.0)	0	0	0	5	10
TOTAL	**60**	**80**	**75**	**75**	**100**
12-month SPI value					
Moderate (SPI < −1.0)	50	75	85	50	65
Severe (SPI < −1.5)	0	5	5	10	25
Extreme (SPI < −2.0)	0	0	0	0	5
TOTAL	**50**	**80**	**90**	**60**	**95**

4.3.3 Extreme flood events

Projected changes in the 90th percentile high-flow days are highly variable for the Medjerda basin. As seen in Figure 26, decreases are projected towards end-century for RCP 4.5. On the other hand, results for RCP 8.5 exhibit increases at mid-century and decreases at end-century. Eventhough this indicator exhibits decreases for RCP 4.5, results for the 100- year flood value project significant increases from 7,890 m^3/s (reference period) to 8,436 m^3/s at mid-century for this emission scenario. For RCP 8.5, mean values decrease over time compared to the reference period, with 7,533 m^3/s and 7,627 m^3/s at mid-century and end-century, respectively (Figure 27 and Table 12).

FIGURE 26: Mean number of 90th percentile high-flow days for different emission scenarios and time periods for the Medjerda River basin

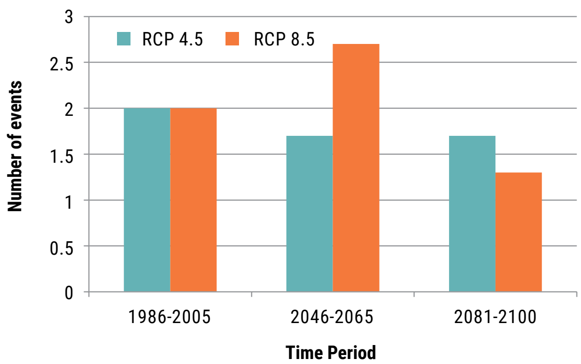

FIGURE 27: Mean change in the 100-year flood value (m^3/s) over time for ensemble of three RCP 4.5 and RCP 8.5 projections for the Medjerda River basin

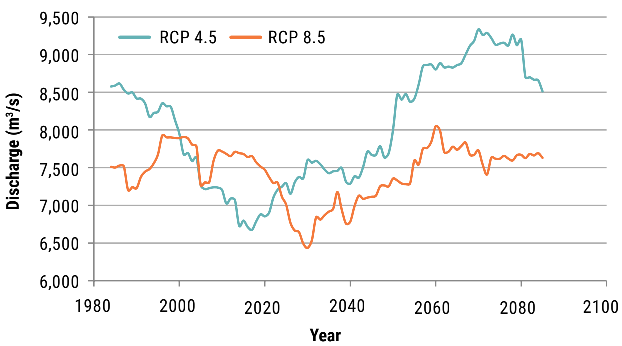

TABLE 12: Mean ensemble 100-year flood values (m^3/s) for different emission scenarios and time periods for the Medjerda River basin

Emission scenario	1986–2005	2046–2065	2081–2100
RCP 4.5	7,890 a	8,436 b	9,031 a
RCP 8.5		7,535 b	7,627 ab

Means followed by different letters indicate statistically significant differences according to the Student's t-test ($p < 0.05$)

5 SUMMARY OF KEY FINDINGS

The findings drawn from the results of this study are summarized below.

For the Nahr el Kabir basin, by the end of the century and for both emission scenarios:

- There is a notable projected increase in heat extremes such as warm-spell duration, number of hot days, number of very hot days, and tropical nights over time;
- Though projected results for precipitation indicators are variable, they indicate an overall increase in precipitation intensity and very heavy precipitation days over time;
- There is a projected tendency towards drier conditions at the end of the century with an increase in the occurrence of moderate drought in particular for RCP 8.5 for the 12-month SPI, but with no severe or extreme droughts events projected to occur;
- The Nahr el Kabir basin is likely to experience increased flood frequencies and a significant increase in the magnitude of peak flow over the 21st century.

For the Wadi Diqah basin:

- There is a significant projected increase in heat extremes such as warm-spell duration, number of hot days, number of very hot days and tropical nights over time and for both emission scenarios;
- Results indicate an overall increase of precipitation intensity and very heavy precipitation days, together with increasing consecutive dry days by the end of the century;
- In accordance with the reference period, there is no indication of projected severe or extreme droughts over the 21st century, while moderate drought conditions are still projected to occur with generally few changes compared to the reference period;
- The basin is likely to experience a progressive general increase in the magnitude of peak flow by the end of the century, together with a decreasing number of extreme flood days at mid-century followed by an increase at end-century.

For the Medjerda basin:

- A significant increase in all heat extremes is projected, such as warm-spell duration, number of hot days, number of very hot days, and tropical nights by the end of the century for both RCPs;
- There is a projected overall decrease in heavy precipitation days over time and for both emission scenarios, together with an increase in consecutive dry days at mid-century for RCP 4.5 and at end-century for the high emission scenario;
- There is a tendency towards significantly drier conditions with projected episodes of severe and extreme droughts in addition to moderate drought over time and for both emission scenarios;
- The Medjerda basin is likely to experience an increase in the magnitude of peak flows for the moderate emission scenario, together with a decreasing number of extreme flood events. For the high-emission scenario, however, the mean magnitude of peak flow is projected to decrease over time.

ENDNOTES

1. WMO, 2011.
2. Fowler et al., 2005 ; Beniston et al., 2007.
3. See ESCWA et al., 2017 for further information.
4. Also referred to as Nahr el Kabir Al-Janoubi (the great southern river), not to be confused with the Nahr el Kabir Al-Shamali (the great northern river), a river in the Syrian Arab Republic that is not shared.
5. See ESCWA et al., 2017 for further information.
6. The full list of extreme events indices can be found at ETCCDI, 2009.
7. Zhang and Yang, 2004. RClimDex was developed and is maintained at the Climate Research Branch of the Meteorological Service of Canada. It provides a graphical user interface to compute the 27 core indices and perform quality control on the input daily data (ETCDDI, 2017).
8. McKee et al., 1993.
9. The Hydrologic Engineering Center Hydrological Modelling System was developed by the US Army Corps of Engineers, 2000.

REFERENCES

Abramowitz, M. and Stegun, I. 1965. Handbook of Mathematical Functions with Formulas, Graphs, and Mathematical Tables. Published by Dover Books on Advanced Mathematics. New York: Dover.

Beniston, M., Stephenson, D. B., Christensen, O. B., Ferro, C., et al. 2007. Future Extreme Events in European Climate: an Exploration of Regional Climate Model Projections. *Climatic Change*, 81: p. 71-95.

Edwards, D. C. and McKee, T. B. 1997. Characteristics of 20th Century Drought in the United States at Multiple Times Scales. *Atmospheric Science Paper*, 634: p. 1-30.

ESCWA (United Nations Economic and Social Commission for Western Asia) et al. 2017. Arab Climate Change Assessment Report – Main Report. Beirut, E/ESCWA/SDPD/2017/RICCAR/Report.

ETCCDI (Expert Team on Climate Change Detection and Indices). 2009. ETCCDI/CRD Climate Change Indices: Definition of the 27 Core Indices. Available at: http://etccdi.pacificclimate.org/list_27_indices.shtml.

ETCCDI (Expert Team on Climate Change Detection and Indices). 2017. Climate Change Indices: Software. Available at: http://etccdi.pacificclimate.org/software.shtml.

Fowler, H. J., Ekstrom, M., Kilsby, C. G. and Jones, P. D. 2005. New Estimates of Future Changes in Extreme Rainfall across the UK Using Regional Climate Model Integrations. 1. Assessment of Control Climate. *Journal of Hydrology*, 300: p. 212-233.

McKee, T. B., Doesken, N. J. and Kleist, J. 1993. The Relationship of Drought Frequency and Duration to Time Scales. *Proceedings of the 8th Conference on Applied Climatology*, 17(22): p. 179-183.

US Army Corps of Engineers. 2000. Hydrologic Modeling System (HEC-HMS). Available at: http://www.hec.usace.army.mil/software/hec-hms/.

WMO (World Meteorological Organization). 2011. World's 10th Warmest year, Warmest Year with La Niña Event, Lowest Arctic Sea Ice Volume. In *Press Release Number: 935.* Geneva. Available at: https://public.wmo.int/en/media/press-release/no-935-2011-world's-10th-warmest-year-warmest-year-la-niña-event-lowest-arctic.

Zhang, X. and Yang, F. 2004. RClimDex (1.0) User Guide. Published by Climate Research Branch Environment Canada. Downsview, Ontario, Canada.